Progress In Electromagnetics Research M, Vol. 139, 11–20, 2026

PIER M

(Received 6 May 2026, Accepted 15 June 2026, Scheduled 20 July 2026)

Using Reverberation Chambers as Test Environments for mmWave Wireless Systems

Alfredo De Leo[1,2,*], Luca Bastianelli[1,2], Valter Mariani Primiani[1,2], Davide Micheli[3], Renzo Lattanzi[3], Pietro Obino[3], Max Moccia[4], Thirumaran Muthiah[4], Riccardo Diamanti[5], and Franco Moglie[1,2]

[1]*Department of Information Engineering, Università Politecnica delle Marche, Via B. Bianche 12, Ancona 60131, Italy*
[2]*Consorzio Nazionale Interuniversitario per le Telecomunicazioni, CNIT, Viale G. P. Usberti 181/A, Parma 43124, Italy*
[3]*Telecom Italia Mobile, TIM, Rome 00198, Italy*
[4]*Cambium Networks, Eastern Road, Ashburton, TQ13 7UP, United Kingdom*
[5]*FiberCop, Via Guido Miglioli 8, Ancona 60131, Italy*

ABSTRACT: This study presents millimeter-wave propagation measurements at 60 GHz conducted in a reverberation chamber to emulate realistic multipath-rich indoor environments. Both line-of-sight (LOS) and non-line-of-sight (NLOS) scenarios are investigated using commercial off-the-shelf devices. The impact of stirring conditions and lossy environments is evaluated through key performance indicators, including Received Signal Strength Indicator (RSSI), Signal-to-Noise Ratio (SNR), Modulation and Coding Scheme (MCS), and throughput. Results show that mechanical stirring speed and the placement of absorbing materials significantly affect channel characteristics and system performance. In NLOS conditions, multipath propagation dominates, where dynamic beamforming demonstrates improved robustness. In contrast, LOS scenarios are highly sensitive to blockage, leading to notable performance degradation. Overall, the findings confirm that the reverberation chamber is an effective platform for over-the-air testing and characterization of 60 GHz wireless systems, offering valuable insights into system behavior under complex indoor propagation conditions relevant to future 5G and 6G deployments.

1. INTRODUCTION

Mobile data traffic continues to grow rapidly, driven by the widespread adoption of smartphones, tablets, and connected devices capable of generating and exchanging zettabytes of data annually [1]. This trend has led to an increasing demand for high-capacity wireless communication systems and the continuous development of new technologies to support emerging applications and services. However, conventional wireless systems operating below 6 GHz face spectrum congestion, limiting their ability to maintain required data rates.

In this context, millimeter-wave (mmWave) frequencies, particularly around 60 GHz, have attracted significant interest because of the large amount of available unlicensed bandwidth. This has motivated extensive research on indoor propagation characteristics, including path loss, fading behavior, and channel modeling, which are essential for the design of high-throughput wireless local area network (WLAN) systems. Previous studies have investigated the spatial and temporal properties of 60 GHz channels, highlighting the strong dependence of signal propagation on environmental factors, antenna directivity, and polarization [2, 3].

Reverberation chambers (RCs) have emerged as powerful tools for over-the-air (OTA) testing and characterization of wireless systems owing to their ability to generate statistically isotropic, rich multipath electromagnetic environments. These properties make RCs particularly suitable for evaluating key performance indicators such as total radiated power (TRP), antenna efficiency, and system-level metrics under controlled yet realistic propagation conditions. Recent studies have demonstrated the extension of RC-based methodologies to millimeter-wave frequencies, supporting their applicability to future 5G and 6G systems [4, 5].

Beyond standard OTA testing, reverberation chambers have been widely investigated for advanced measurement techniques and wireless channel emulation. For instance, reflectivity measurements based on absorption cross-section (ACS) analysis have shown that measurement uncertainty is primarily determined by the number of independent samples collected in the chamber [6]. Moreover, the efficiency of mechanical stirring and identification of uncorrelated field configurations have been studied using multivariate statistical approaches, emphasizing the importance of accurate field characterization in RC environments [7].

RCs have also been employed to emulate realistic wireless propagation scenarios and assess the performance of communication systems under controlled multipath conditions. The impact of retransmission mechanisms in wireless systems, such as ZigBee, has been analyzed in variably loaded chambers, demonstrating the strong influence of multipath richness on the packet error rate and system reliability [8]. Additionally, the practical aspects of channel emulation, including delay spread and chamber loading, have been investigated to better reproduce real-world propagation environments [9].

* Corresponding author: Alfredo De Leo (a.deleo@univpm.it).

doi:10.2528/PIERM26050607

Published by THE ELECTROMAGNETIC ACADEMY

In the field of antenna measurements, reverberation chambers have been used to evaluate multi-element antenna systems, where limited independent channel samples may introduce a bias in the estimation of the diversity gain and channel capacity [10]. Furthermore, RCs have proven effective for assessing antenna performance in realistic scenarios, such as on-body wearable systems, where human-body interactions significantly affect radiation efficiency and overall performance [11].

Compared to anechoic chambers, which provide a deterministic free-space environment suitable for antenna characterization and beamforming analysis, reverberation chambers generate a statistically isotropic and dynamically varying multipath environment. This makes them particularly suitable for evaluating system-level performance metrics such as throughput, robustness, and adaptive behavior under fading conditions. Therefore, the two approaches are complementary: anechoic chambers are ideal for link budget and radiation analysis, while reverberation chambers enable repeatable testing under realistic and challenging propagation conditions, which are especially relevant for mmWave systems.

The present work provides an extensive experimental investigation of 60 GHz propagation in a reverberation chamber, with the aim of replicating complex multipath-rich indoor wireless environments. Both line-of-sight (LOS) and non-line-of-sight (NLOS) scenarios are considered, using commercial off-the-shelf (COTS) devices to ensure practical relevance. This study focuses on the impact of mechanical stirring conditions and the introduction of absorbing materials on key system-level metrics, including the Received Signal Strength Indicator (RSSI), Signal-to-Noise Ratio (SNR), Modulation and Coding Scheme (MCS), and throughput.

With respect to the state of the art [12], typically focuses on RC testing of wireless antennas using base stations and user equipment emulators, the present paper is based on a commercial off-the-shelf client-server system, which integrates antennas, without the need of external emulators.

The results highlight the critical roles of stirring dynamics and chamber loading in shaping the propagation channel. In LOS configurations, the presence of obstructions along the direct path leads to significant performance degradation, thereby emphasizing the importance of maintaining clear propagation conditions. Conversely, in NLOS scenarios, multipath propagation dominates, resulting in enhanced channel richness, where adaptive techniques such as beamforming demonstrate increased robustness.

2. MEASUREMENT SYSTEM DESCRIPTION

The measurement system consisted of a transmitter and a receiver, both configured to operate in the frequency range of 61.56 GHz to 63.72 GHz, placed in a reverberation chamber. These three components are described in the following subsections.

2.1. Reverberation Chamber

The reverberation chamber used in the test was a rectangular cavity made of galvanized steel with dimensions of $6 \times 4 \times 2.5\,\mathrm{m}^3$. The stirring action was achieved by rotating a mechanical stirrer with a horizontal axis and eight irregular metallic plates [13]. Owing to its physical dimensions, the RC has its first resonance mode at 45 MHz and its Lowest Usable Frequency (LUF) around 300 MHz, thus facing uniformity and anisotropy constraints provided by [14]; this means that the RC is well overmoded at the working frequencies of the transmitting and receiving devices.

In addition to being a facility for electromagnetic compatibility (EMC) tests, the RC allows us to emulate real-life propagation conditions [15, 16] for testing wireless systems [17–19]. Figure 1 shows a picture of the chamber during the characterization tests, performed using a vector network analyzer (VNA) and two V-band horn antennas, using the WR-15 waveguide standard, well matched in the 50 GHz to 75 GHz millimeter-wave frequency range and with a gain of 24 dBi, horizontal beam-with = 11°, vertical beam-with = 9.5° [20].

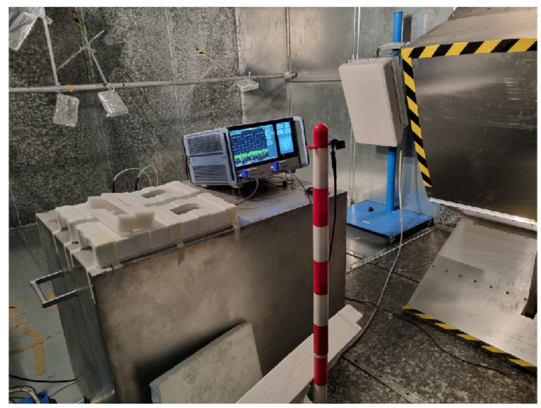

FIGURE 1. Reverberation chamber and the setup used for its characterization.

The quality factor (Q), calculated according to Eq. (1) [14], is reported in Figure 2.

$$\mathrm{Q} = \frac{16\pi^2 V}{\eta_{Tx}\eta_{Rx}\lambda^3} < |S_{21}|^2 > \tag{1}$$

where V is the chamber volume (m^3); λ is the wavelength (m); η_{Tx} and η_{Rx} are the total antenna efficiency factors for the transmitting and receiving antennas, respectively.

Two indicators of RC are useful to compare it with a wireless propagation environment: The first is the Rician K factor (K) [21], given as the ratio between the power of the direct path and the power of the scattered components (2).

$$\mathrm{K} = \frac{(|< S_{21} >_N|)^2}{(|S_{21} - < S_{21} >_N|)^2} \tag{2}$$

where the angle brackets represent the averaging operator over the N stirrer positions.

Figure 3 shows that, at these frequencies, the reverberation chamber does not exhibit ideal behavior, as K-factor values lower than unity are expected.

This meant the presence of static multipath behavior of the test site, and the measured K-factor remained consistent with

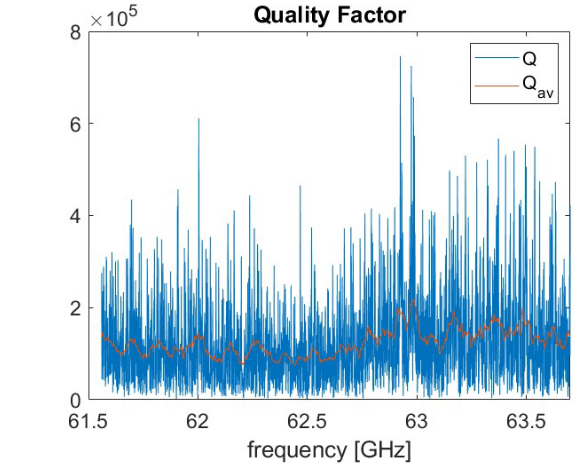

FIGURE 2. Quality factor of the reverberation chamber in the frequency range 61.56 GHz–63.72 GHz.

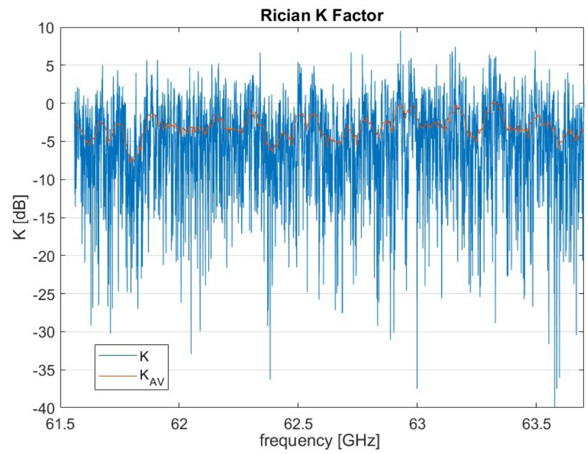

FIGURE 3. Rician K-factor of the reverberation chamber.

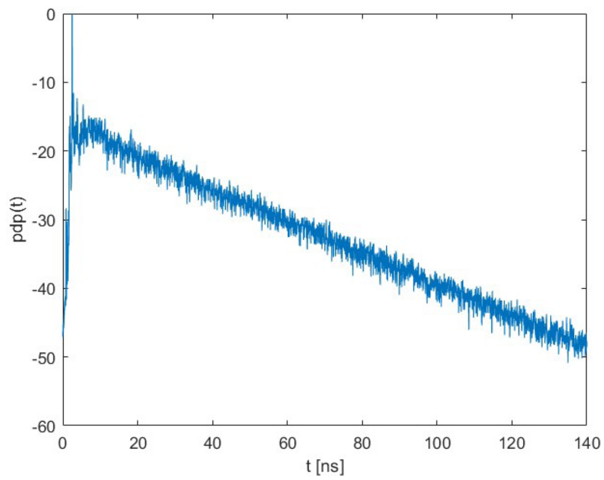

FIGURE 4. Power delay profile of the reverberation chamber.

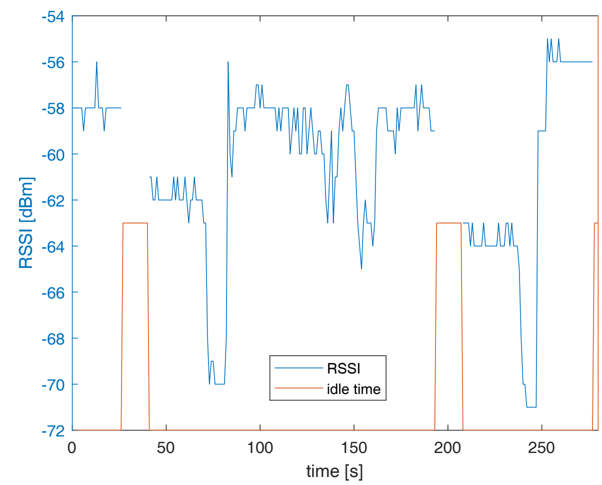

FIGURE 5. Measurement of the RSSI parameter for 280 seconds.

those observed in realistic wireless propagation environments [22–24].

The second is the power delay profile (PDP), which is the measured power response of a signal as a function of time delay and is calculated by applying the -20 dB threshold [25, 26], according to Eq. (3)

$$\text{PDP(t)} = < |IFT(S_{21}(f)|^2 >_N \tag{3}$$

where IFT denotes the Inverse Fourier Transform of the frequency domain waveform of $S_{21}(f)$, and angle brackets denote the ensemble average over the N stirrer positions.

This parameter is shown in Figure 4. From the time-domain waveform of the PDP, a root-mean-square (RMS) delay spread of $\tau_{RMS} = 81$ ns was obtained, which is in agreement with those reported in the literature for wireless scenarios in mm-wave frequency ranges [2, 3].

2.2. Transmitting and Receiving Devices

During the tests, two COTS devices were used: a cnWaveTM V1000 unit [27] as a transmitter and a cnWaveTM V5000 unit [28] as a receiver. The main characteristics of the equipment are summarized in Tables 1 and 2, respectively. The beamforming functionality remained enabled during the tests for both devices.

During all tests, both the V1000 and V5000 were placed inside the RC, and their performance is monitored by a laptop placed outside the RC and connected to them via optical fiber. The key performance indicators (KPIs) are monitored by the V5000 and collected by the laptop through simple network management protocol (SNMP) queries. The KPIs are reported in Table 3, which also includes a short description and their units, omitted in the next tables for space considerations.

Figure 5 reports an example of the time-domain measurement of the RSSI parameter (blue line) and the corresponding idle times (red line), which occur when the connection between the server and the client is down. It must be remarked that the RSSI is an indicator related to the power measurement in dBm on the received management packets only, and not on all the data exchanged between client and server. If the transmitting power is known, the RSSI can be used to compute the signal attenuation due to the propagation environment.

TABLE 1. CN V1000 features.

Frequency Range	57 to 66 GHz
Channel Width	2.16 GHz
Modulation Coding Schemes	MCS-0 to MCS-10
Maximum EIRP	38 dBm
Gain	22.5 dBi
Beamforming Scan Range	±40 deg azim., ±20 deg elev.
Beam Width	12 deg

TABLE 2. CN V5000 features.

Frequency Range	57 to 66 GHz
Channel Width	2.16 GHz
Modulation Coding Schemes	MCS-0 to MCS-12
Maximum EIRP	38 dBm
Gain	22.5 dBi
Beamforming Scan Range	±140 deg azim., ±20 deg elev.
Beam Width	12 deg

TABLE 3. Monitored key performance indicators.

EIRP [dBm]	Equivalent Isotropically Radiated Power: is a measurement of radiated output power from an ideal isotropic antenna.
RSSI [dBm]	Receive Signal Strength Indicator: is a measurement of the power present in a received radio signal, measured during management packets every 25.6 ms.
MCS	Modulation Coding Schemes: is a metric that describes how data is encoded and transmitted over a wireless connection.
SNR [dB]	Signal to Noise Ratio: is a measurement of the level of a desired signal over the level of background noise, measured during management packets every 25.6 ms.
T_xByteRate [byte/s]	Throughput in transmission.
T_x elev. [deg]	Transmission elevation angle
T_x azim. [deg]	Transmission azimuth angle
R_x elev. [deg]	Reception elevation angle
R_x azim. [deg]	Reception azimuth angle
Idle Time [s]	Time with no connection

3. RESULTS

This section presents the experimental results obtained from the measurement campaign conducted in the reverberation chamber under different propagation conditions. The analysis focuses on KPIs, including RSSI, SNR, MCS, throughput, and idle time, evaluated in both LOS and NLOS configurations with and without the presence of lossy materials.

During the test reported in this study, the stirrer was continuously rotated (stirring mode). Preliminary tests were conducted using the reverberation chamber (RC) in step mode. The evaluated client–server system, however, operates with beamforming permanently enabled; consequently, it automatically reconfigured the transmission and reception angles as a function of the stirrer position, in step mode. Therefore, the stirring mode represents a more hostile condition for the test of the system. In fact, this condition imposes a more demanding test, as it more strongly challenges the system's capability to dynamically adapt to time-varying scenarios.

3.1. LOS Lossless Configuration

LOS configuration was the first scenario explored during the tests because it is the most widely used configuration, in both point-to-point and point-to-multipoint systems.

Figure 6 shows the LOS setup in RC: V1000 and V5000 are placed in line of sight, and the horizontal stirrer, which rotates with angular speed ω, is placed between the transmitter and receiver. The vertical stirrer and metallic box remained stationary and acted as scattering objects.

However, the horizontal stirrer rotated during the tests and simulated the effect of a moving object interposed between the transmitter and receiver. In a realistic outdoor scenario, for example, a bus passes on a street. As an example of how the stirrer affects the performance of the V1000-V5000 connection, Figure 7 shows how the RSSI varies when the horizontal stirrer is moved at two different angular speeds $\omega_1 = 2$ deg/s and $\omega_2 = 5$ deg/s. The different rotating speeds affected both the periodicity of the RSSI pattern and its average value. The effect of ω on other parameters was also investigated for the three different speeds.

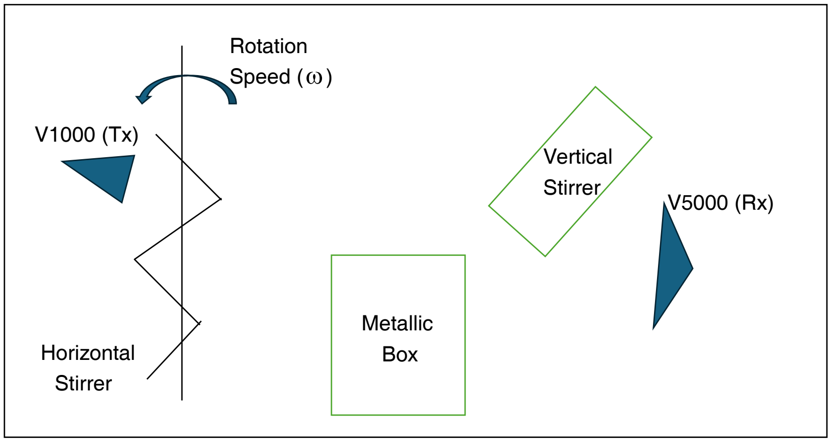

FIGURE 6. Line of sight lossless scenario.

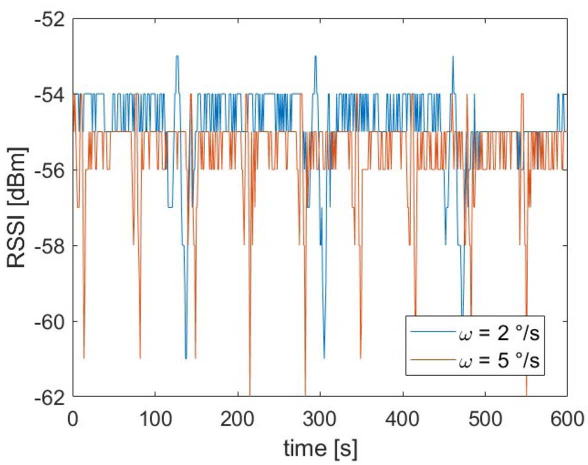

FIGURE 7. RSSI fluctuations with two rotation angular speeds of the horizontal stirrer.

TABLE 4. LOS scenario, $\omega = 2$ deg/s no losses.

	RSSI	SNR	MCS	TxByteRate
max	-53	20	8	$1.22\,10^8$
min	-62	12	8	$1.33\,10^3$
avg	-55.69	17.99	8	$1.20\,10^8$
std [dB]	0.82	0.81	0	0.41
idle time = 0 s				

Tables 4, 5, and 6 report the statistical analysis of the RSSI, SNR, MCS, and TxByteRate, respectively, during a test in which the stirrer continuously rotated at angular speed of $\omega = 2$ deg/s, $\omega = 5$ deg/s, and $\omega = 10$ deg/s, respectively; during these tests, the EIRP remained fixed at 13 dBm, and no lossy material was introduced into the RC.

Although the beamforming function was active, no variation in T_x/R_x elevation or azimuth angles was observed, and no idle times were observed throughout the testing period.

When comparing the performance at the three different rotation speeds, it can be observed that they do not significantly affect the RSSI, SNR, and MCS; only the minimum through-

TABLE 5. LOS scenario, $\omega = 5$ deg/s no losses.

	RSSI	SNR	MCS	TxByteRate
max	-54	20	9	$1.22\,10^8$
min	-62	11	8	$1.52\,10^3$
avg	-55.76	17.89	8.01	$1.20\,10^8$
std [dB]	0.83	0.79	0.04	0.39
idle time = 0 s				

TABLE 6. LOS scenario, $\omega = 10$ deg/s no losses.

	RSSI	SNR	MCS	TxByteRate
max	-54	20	8	$1.22\,10^8$
min	-62	12	8	$4.22\,10^6$
avg	-55.7	17.9	8	$1.20\,10^8$
std [dB]	0.83	0.78	0	0.42
idle time = 0 s				

put, in correspondence to the shadowing effect of the stirrer, is lower for lower ω values. This fact is ascribed to the logic of the system firmware, which reduces the transmission rate in the event that obstacles are present for longer periods of time at lower ω between the transmitter and receiver.

3.2. Line-of-Sight Lossy Configuration

The LOS scenario described in the previous subsection was also explored in a lossy configuration by adding a VHP-8-NRL absorbing panel in two different positions (Figure 8). In the first position, the lossy panel intercepts the line between V1000 and V5000, whereas in the second position, the panel is placed out of the line-of-sight. Table 7 reports the KPIs for lossless and two lossy configurations. It can be observed that, as expected, the losses reduce the received power and also slightly decrease the SNR. However, losses slightly increase throughput, as the system sets a higher value for the MCS. This can be explained by considering that the lower the quality factor, the fewer the multipath conditions. From a system perspective, the multipath acts as a source of interference in the case of a dominant

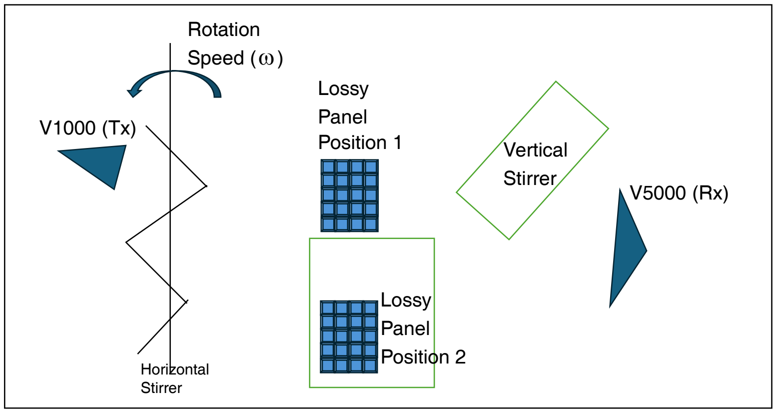

FIGURE 8. Line-of-sight lossy scenario.

TABLE 7. LOS scenario, $\omega = 2$ deg/s — Effect of losses.

Metric	Lossless	1 el., pos. 1	1 el., pos. 2
RSSI [dBm]			
max	-53	-54	-55
min	-62	-62	-65
avg	-55.69	-56.33	-57.8
std	0.82	0.84	0.95
SNR [dB]			
max	20	20	19
min	12	11	9
avg	17.99	17.29	15.85
std	0.81	0.85	1
MCS			
max	8	9	9
min	8	7	9
avg	8	8.29	9
std	0	0.32	0
TxByteRate [byte/s]			
max	$1.22 \cdot 10^8$	$1.26 \cdot 10^8$	$1.26 \cdot 10^8$
min	$1.33 \cdot 10^3$	$1.25 \cdot 10^3$	$4.22 \cdot 10^7$
avg	$1.20 \cdot 10^8$	$1.20 \cdot 10^8$	$1.24 \cdot 10^8$
std	0.41	0.47	0.31

line-of-sight scenario. This consideration is confirmed by the higher MCS values adopted by the system in the case of the lossy panel placed in position 2, which reduces the multipath effect with respect to position 1, not in the line of sight between the transmitter and receiver.

3.3. NLOS Lossless Configuration

In real-life situations, both indoors and in urban environments, it may also be interesting to investigate the NLOS configuration to analyze the maximum extension of the system radio coverage. The RC is well suited to emulate this situation because the reverberation environment enhances the multipath, and the direct path can be strongly reduced by proper antenna orientation and obstacle(s) positioning. We placed the devices in a back-

TABLE 8. NLOS scenario, $\omega = 2$ deg/s No lossy panels.

	RSSI	SNR	MCS	TxByteRate
max	-55.87	17.75	6.75	$9.74\,10^7$
min	-70.62	0.5	2	$2.11\,10^7$
avg	-58.84	14.77	4.4	$6.21\,10^7$
std	1.83	1.90	1.46	1.64
idle time: 10.25 s over 2400 s				

TABLE 9. NLOS scenario, $\omega = 5$ deg/s No lossy panels.

	RSSI	SNR	MCS	TxByteRate
max	-55	18.87	8.125	$1.14\,10^8$
min	-71.25	-0.87	2	$2.37\,10^7$
avg	-58.48	15.15	4.771	$6.81\,10^7$
std	2.18	2.24	1.93	1.67
idle time: 29.375 s over 2400 s				

to-back configuration, as shown in Figure 9. In this way, the direct path between the transmitter and receiver is minimized, considering the wide beamforming scan range provided by the V5000. In addition, to minimize the direct link, the transmitter points towards the horizontal stirrer, and the receiver is pointed to the opposite direction with respect to the V1000 and metallic box, whereas the still vertical stirrer acts as diffusers. In this scenario, the multipath effect introduced by the RC is fundamental. In the first set of measurements, no lossy panels were inserted into the RC, and the resonant characteristics of the environment were emphasized. During these tests, the EIRP was fixed at 13 dBm. The NLOS scenario is a more hostile environment than the LOS scenario. Therefore, during the tests, we observed variations in T_x/R_x elevation or azimuth angles and idle times.

Tables 8, 9, and 10 report the statistical analysis of RSSI, SNR, MCS, and T_xByteRate, respectively, during tests in which the stirrer rotates at angular speeds $\omega = 2$ deg/s, $\omega = 5$ deg/s, and $\omega = 10$ deg/s, respectively. Tests with an angular velocity of 2 deg/s emulate an obstacle that moves very slowly and rarely blinds the system. The tests with an angular velocity of 10 deg/s, on the other hand, represent obstacles that blind the

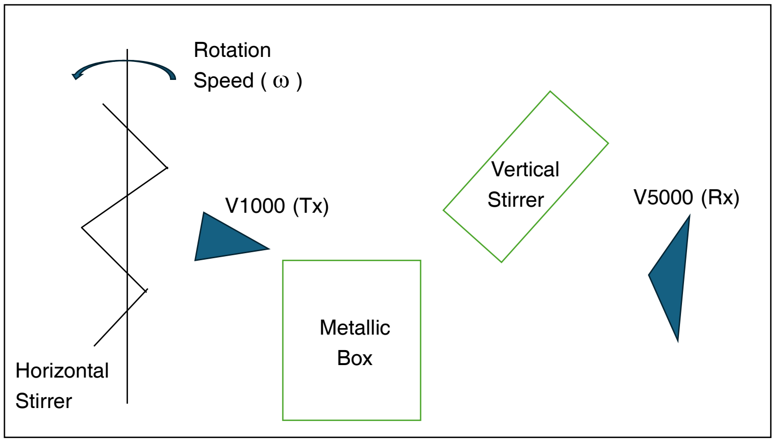

FIGURE 9. Non-line-of-sight lossless scenario.

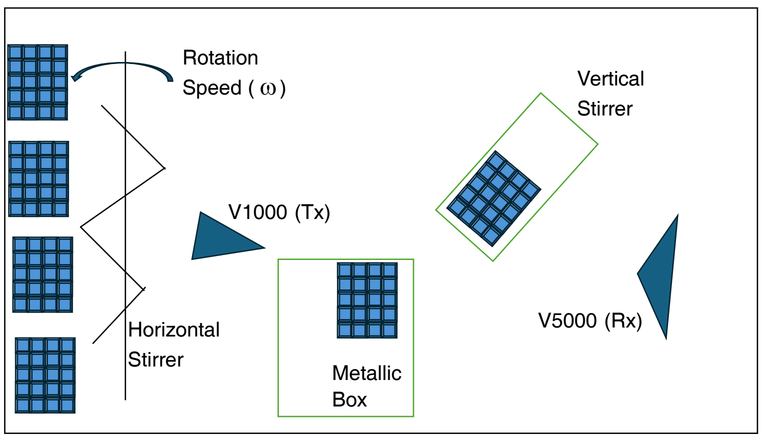

FIGURE 10. Non-line-of-sight lossy scenario.

TABLE 10. NLOS scenario, $\omega = 10$ deg/s No lossy panels.

	RSSI	SNR	MCS	TxByteRate
max	-55.75	18	3.75	$4.76\,10^7$
min	-70.87	0.125	2	$2.30\,10^7$
avg	-58.48	15.15	2.40	$3.72\,10^7$
std	1.55	1.61	0.88	0.69
idle time: 4 s over 2400 s				

system for shorter periods but more frequently. The tests at an angular velocity of 5 deg/s represent an intermediate case.

When transitioning from $\omega = 2$ deg/s to $\omega = 5$ deg/s, the system responds by increasing MCS, consequently the throughput. However, when switching from $\omega = 5$ deg/s to $\omega = 10$ deg/s, the system perceives a hostile propagation environment because idle events become more frequent. As a consequence, the system adapts itself by reducing the MCS and transmission speed, thus ensuring better connection stability and, consequently, reducing idle times. For the tested devices and used configuration, the system response is not strictly proportional to the speed of the moving obstacle. A similar behavior was observed for systems working in the 2.45 GHz band [29]. In addition, comparing the system performance with the LOS scenario in Subsection 3.1, we note lower values of MCS and throughput, but characterized by a lower spread. This can be explained considering that in the LOS scenario the connection is mainly due to a single direct path. When the stirrer intercepts this path, it causes a strong degradation in performance. On the other hand, in the NLOS scenario, the connection is due to a larger number of paths, and the stirrer can negatively affect only some of them.

3.4. Non-Line-of-Sight Lossy Configuration

It is interesting to investigate the effect of the insertion of lossy elements into the RC in the NLOS scenario because losses affect the scattered component of the electromagnetic field, which plays a more relevant role in the LOS scenario. In this study, six absorbing panels were inserted into the RC, as shown in Figure 10.

Table 11 reports the effect of the losses on the performance of the tested system. With respect to RSSI, losses increase its maximum value and decrease the minimum value. This can be explained by considering that the RSSI is a measurement of the received power related only to the useful component of the signal. Depending on the position of the stirrer, the best case occurs when most of the signal travels from the transmitter to

TABLE 11. NLOS scenario, $\omega = 2$ deg/s effect of Losses.

	RSSI		SNR	
	lossless	6 panels	lossless	6 panels
max	-55.87	-54.37	17.75	19.62
min	-70.62	-72.5	0.5	-5.37
avg	-58.84	-57.85	14.77	15.80
std	1.83	2.41	1.90	2.46
	MCS		**TxByteRate**	
	lossless	6 panels	lossless	6 panels
max	6.75	9	$9.74\,10^7$	$1.31\,10^8$
min	2	2	$2.11\,10^7$	$6.17\,10^6$
avg	4.4	7.55	$6.21\,10^7$	$8.94\,10^7$
std	1.46	1.52	1.64	1.61
idle time: 10.25 s (lossless) 11.5 s (6 panels) over 2400 s				

the receiver after multiple reflections are not intercepted by the stirrer elements (paddles of the metallic stirrer in Figure 1). By contrast, the worst case is the one in which most of the power is intercepted by the stirrer.

In the best cases, the power from the multipath as a result of the electromagnetic field stirred by the RC is seen by the system as noise. Therefore, the SNR increases in the case of a lossy scenario. In the worst cases, the signal is mainly due to the scattered part of the electromagnetic wave, and losses lower this component. For the same reason, in the best-case scenario, the system increases the MCS and consequently the transmission rate. In fact, losses reduce the scattered component of the power; therefore, we observed higher values of MCS and TxByteRate in the lossy configuration. A larger spread between the performance in the best and worst case scenarios can also be observed in terms of higher values of the standard deviation of all monitored parameters, with respect to the lossless configuration.

4. DISCUSSION ON RESULTS

The experimental results highlight several important aspects of wireless system behavior at 60 GHz, while also providing insight into the role of the reverberation chamber (RC) as a testing environment.

Although the RC used in this study does not fully exhibit the characteristics of an ideal reverberation environment, as indicated, for example, by the non-ideal Rician K-factor values, it nevertheless proves to be a highly effective platform for testing wireless systems under challenging and dynamic propagation conditions.

In LOS scenarios, the system performance is strongly dependent on the presence of a stable direct path. The measurements show that variations in stirring speed have limited impact on the average KPI values (RSSI, SNR, MCS) but significantly affect the temporal fading behavior and minimum throughput. This indicates that even under non-ideal reverberation conditions, the RC can reproduce realistic obstruction effects, mimicking moving objects that intermittently block the link.

The introduction of lossy materials in LOS configurations further demonstrates that the RC can emulate propagation impairments beyond simple multipath effects. While attenuation reduces the received power, it can also improve transmission efficiency by limiting multipath interference, leading to higher MCS levels. This confirms that the chamber environment, even if not perfectly isotropic, allows for meaningful observation of interference-related phenomena.

The importance of multipath propagation becomes evident in NLOS scenarios. Despite the non-ideal reverberation properties, the RC successfully creates a sufficiently rich scattering environment to sustain communication in the absence of a direct path. The system response to different stirring speeds showed nonlinear adaptation, with moderate dynamics improved performance, whereas excessive dynamics led to instability and increased idle times. This shows that RC can effectively reproduce harsh and time-varying channel conditions in the real world.

When lossy elements are introduced in NLOS configurations, their impact becomes more critical. Because communication relies on scattered components, attenuation can enhance and degrade performance depending on the instantaneous channel realization. The observed increase in KPI variability confirms that the RC can generate highly fluctuating and stressful propagation scenarios, which are particularly relevant for robustness testing.

Regarding wireless system tests in RCs at lower frequencies, it has been reported that system performance under stirred conditions is governed by multipath richness and temporal fading, leading to fluctuations in key performance indicators, such as throughput and modulation schemes. For example, in [29], this behavior was observed for WLAN systems operating at 2.4 GHz, where moderate channel dynamics improve performance, while excessive dynamics degrade link stability. Our results at 60 GHz are consistent with these findings, while also highlighting frequency-specific effects. In particular, similarly to lower-frequency studies, we observe that the system adapts to channel variations by adjusting the modulation and coding scheme (MCS), confirming the validity of RC-based testing across frequencies. However, at 60 GHz, the impact of blockage and beamforming is significantly more pronounced. In LOS scenarios, the performance degradation caused by obstruction of the direct path is stronger than typically observed at lower frequencies. In NLOS conditions, the role of multipath becomes critical, and the RC environment successfully reproduces a sufficiently rich scattering scenario to sustain communication, consistent with observations at lower frequencies [8]. The non-linear relationship between stirrer speed and throughput observed in our measurements is also in agreement with previous studies at lower frequencies [29], where excessive channel dynamics lead to increased instability and idle periods. As regards the effect of the positioning of lossy elements, in the case of LTE-4G frequencies (1.8 GHz band) [30], they increase the system throughput regardless of their position. This can be ascribed to the fact that at these frequencies, the RC has an ideal behavior. On the contrary, at mmWave frequencies we observed a similar effect if the losses do not intercept the main beam, while they reduce the throughput if placed along the main path. This means that the static multipath effect in the RC is dominant, and this assumption is confirmed by higher values of the Rician-K factor.

Overall, although the chamber does not behave as an ideal reverberation environment, the results clearly show that it functions as a valuable and controllable hostile test site for wireless propagation. It enables the emulation of adverse conditions, such as blockage, fading, and reduced multipath diversity, providing a practical and repeatable framework for evaluating system resilience in realistic deployment scenarios.

5. CONCLUSION

This study has demonstrated the effectiveness of a reverberation chamber as a controlled and repeatable environment for evaluating the performance of commercial 60 GHz wireless systems under realistic propagation conditions. Through an extensive experimental campaign, both line-of-sight (LOS) and non-line-of-sight (NLOS) scenarios were analyzed, considering the effects of mechanical stirring dynamics and the introduction of lossy materials.

The results show that in LOS configurations, the system performance is highly dependent on the integrity of the direct path. Obstructions or absorbing elements along this path lead to significant degradation of key performance indicators such as RSSI and SNR. In contrast, under NLOS conditions, where communication is primarily based on multipath propagation, the system exhibits increased robustness due to the availability of multiple propagation paths and the adaptive capabilities of beamforming techniques.

This study also highlights the dual roles of losses within the propagation environment. In LOS scenarios, the introduction of absorbing materials can improve the performance by reducing multipath-induced interference. However, in NLOS configurations, where scattered components are essential for maintaining connectivity, excessive losses can degrade the system performance by attenuating useful signal contributions.

In general, the findings confirm that reverberation chambers provide a valuable platform for over-the-air testing and channel emulation at mm-wave frequencies, enabling a systematic investigation of complex propagation effects.

REFERENCES

[1] Li, Y., J. Yang, and N. Ansari, "Cellular smartphone traffic and user behavior analysis," in *2014 IEEE International Conference on Communications (ICC)*, 1326–1331, Sydney, NSW, Australia, 2014.

[2] Xu, H., V. Kukshya, and T. S. Rappaport, "Spatial and temporal characteristics of 60-GHz indoor channels," *IEEE Journal on Selected Areas in Communications*, Vol. 20, No. 3, 620–630, 2002.

[3] Wu, X., C.-X. Wang, J. Sun, J. Huang, R. Feng, Y. Yang, and X. Ge, "60-GHz millimeter-wave channel measurements and modeling for indoor office environments," *IEEE Transactions on Antennas and Propagation*, Vol. 65, No. 4, 1912–1924, 2017.

[4] Hubrechsen, A., S. J. Verwer, A. C. F. Reniers, L. A. Bronckers, and A. B. Smolders, "Pushing the boundaries of antenna-efficiency measurements towards 6G in a mm-Wave reverberation chamber," in *2021 IEEE Conference on Antenna Measurements & Applications (CAMA)*, 263–265, Antibes Juan-les-Pins, France, 2021.

[5] Fall, A. K., P. Besnier, C. Lemoine, M. Zhadobov, and R. Sauleau, "Design and experimental validation of a mode-stirred reverberation chamber at millimeter waves," *IEEE Transactions on Electromagnetic Compatibility*, Vol. 57, No. 1, 12–21, 2015.

[6] Gifuni, A., H. Khenouchi, and G. Schirinzi, "Performance of the reflectivity measurement in a reverberation chamber," *Progress In Electromagnetics Research*, Vol. 154, 87–100, 2015.

[7] Gradoni, G., V. M. Primiani, and F. Moglie, "Reverberation chamber as a multivariate process: FDTD evaluation of correlation matrix and independent positions," *Progress In Electromagnetics Research*, Vol. 133, 217–234, 2013.

[8] Staniec, K., "Evaluation of the ZigBee transmission repetition mechanism in the variably-loaded reverberation chamber," *Progress In Electromagnetics Research*, Vol. 132, 297–314, 2012.

[9] Pomianek, A. J., K. Staniec, and Z. Joskiewicz, "Practical remarks on measurement and simulation methods to emulate the wireless channel in the reverberation chamber," *Progress In Electromagnetics Research*, Vol. 105, 49–69, 2010.

[10] Chen, X., "Measurements and evaluations of multi-element antennas based on limited channel samples in a reverberation chamber," *Progress In Electromagnetics Research*, Vol. 131, 45–62, 2012.

[11] Soh, P. J., S. J. Boyes, G. Vandenbosch, Y. Huang, and S. L. Ooi, "On-body characterization of dual-band all-textile PIFA," *Progress In Electromagnetics Research*, Vol. 129, 517–539, 2012.

[12] Duan, S., W. Wang, B. Tang, Y. Wu, and Y. Liu, "A review of over-the-air testing methods for performance measurement of antennas and devices in communication systems," *International Journal of RF and Microwave Computer-Aided Engineering*, Vol. 2024, No. 1, 6660144, 2024.

[13] Arnaut, L. R., F. Moglie, L. Bastianelli, and V. M. Primiani, "Helical stirring for enhanced low-frequency performance of reverberation chambers," *IEEE Transactions on Electromagnetic Compatibility*, Vol. 59, No. 4, 1016–1026, 2017.

[14] International Electrotechnical Commission (IEC), "Electromagnetic compatibility (EMC) — Part 4-21: Testing and measurement techniques - Reverberation chamber test methods," IEC, Geneva, Switzerland, 2011.

[15] Bastianelli, L., L. Giacometti, V. M. Primiani, and F. Moglie, "Effect of absorber number and positioning on the power delay profile of a reverberation chamber," in *2015 IEEE International Symposium on Electromagnetic Compatibility (EMC)*, 422–427, Dresden, Germany, 2015.

[16] De Leo, A., P. Russo, and V. M. Primiani, "Emulation of the rician K-factor of 5G propagation in a source stirred reverberation chamber," *Electronics*, Vol. 12, No. 1, 58, 2023.

[17] Bastianelli, L., R. Diamanti, E. Colella, V. M. Primiani, F. Moglie, M. A. Toubal, M. Odit, J.-B. Gros, Y. Nasser, G. Lerosey, *et al.*, "Measurements of reconfigurable intelligent surface in 5G system within a reverberation chamber at MmWave," in *2024 18th European Conference on Antennas and Propagation (EuCAP)*, 1–4, Glasgow, United Kingdom, 2024.

[18] Barazzetta, M., D. Micheli, L. Bastianelli, R. Diamanti, M. Totta, P. Obino, R. Lattanzi, F. Moglie, and V. M. Primiani, "A comparison between different reception diversity schemes of a 4G-LTE base station in reverberation chamber: A deployment in a live cellular network," *IEEE Transactions on Electromagnetic*

Compatibility, Vol. 59, No. 6, 2029–2037, 2017.

[19] Micheli, D., M. Barazzetta, C. Carlini, R. Diamanti, V. M. Primiani, and F. Moglie, "Testing of the carrier aggregation mode for a live LTE base station in reverberation chamber," *IEEE Transactions on Vehicular Technology*, Vol. 66, No. 4, 3024–3033, 2017.

[20] Pasternack, "Wr-15 waveguide standard gain horn antenna," https://www.pasternack.com/single-antenna-operates-from-50-75-GHz-with-a-nominal-dbi-gain-wr-15-input-connectors-pe9881-24-p.aspx, 2026.

[21] Holloway, C. L., D. A. Hill, J. M. Ladbury, P. F. Wilson, G. Koepke, and J. Coder, "On the use of reverberation chambers to simulate a Rician radio environment for the testing of wireless devices," *IEEE Transactions on Antennas and Propagation*, Vol. 54, No. 11, 3167–3177, 2006.

[22] Doukas, A. and G. Kalivas, "Rician K factor estimation for wireless communication systems," in *2006 International Conference on Wireless and Mobile Communications (ICWMC'06)*, 69–69, Bucharest, Romania, 2006.

[23] Zhu, S., T. S. Ghazaany, S. M. R. Jones, R. A. Abd-Alhameed, J. M. Noras, T. V. Buren, J. Wilson, T. Suggett, and S. Marker, "Probability distribution of rician k-factor in urban, suburban and rural areas using real-world captured data," *IEEE Transactions on Antennas and Propagation*, Vol. 62, No. 7, 3835–3839, 2014.

[24] Medawar, S., P. Händel, and P. Zetterberg, "Ricean K-factor estimation and investigation of urban wireless measurements," in *2012 IEEE International Conference on Wireless Information Technology and Systems (ICWITS)*, 1–4, Maui, HI, USA, 2012.

[25] Holloway, C. L., M. G. Cotton, and P. McKenna, "A model for predicting the power delay profile characteristics inside a room," *IEEE Transactions on Vehicular Technology*, Vol. 48, No. 4, 1110–1120, 1999.

[26] Pomianek, A. J., K. Staniec, and Z. Jóskiewicz, "On the use of reverberation chamber to simulate the power delay profile of a wireless channels," in *9th International Symposium on EMC Joint with 20th International Wroclaw Symposium on EMC, EMC Europe 2010*, 245–249, Wroclaw, Poland, 2010.

[27] Cambium Networks, "60 GHz cnWave V1000 client node," https://www.cambiumnetworks.com/products/cnwave/60-ghz-cnwave-v1000/, 2025.

[28] Cambium Networks, "60 GHz cnWave V5000 server node," https://www.cambiumnetworks.com/products/cnwave/60-ghz-cnwave-v5000/, 2025.

[29] Recanatini, R., F. Moglie, and V. M. Primiani, "Performance and immunity evaluation of complete WLAN systems in a large reverberation chamber," *IEEE Transactions on Electromagnetic Compatibility*, Vol. 55, No. 5, 806–815, Oct. 2013.

[30] Micheli, D., M. Barazzetta, F. Moglie, and V. M. Primiani, "Power boosting and compensation during OTA testing of a real 4G LTE base station in reverberation chamber," *IEEE Transactions on Electromagnetic Compatibility*, Vol. 57, No. 4, 623–634, 2015.